4498–4507 *Nucleic Acids Research, 2009, Vol. 37, No. 13* *Published online 27 May 2009*
doi:10.1093/nar/gkp437

High-affinity triplex targeting of double stranded DNA using chemically modified peptide nucleic acid oligomers

Mads E. Hansen, Thomas Bentin and Peter E. Nielsen*

Department of Cellular and Molecular Medicine, University of Copenhagen, Blegdamsvej 3, Copenhagen 2200-N, Denmark

Received February 24, 2009; Revised May 8, 2009; Accepted May 11, 2009

ABSTRACT

While sequence-selective dsDNA targeting by triplex forming oligonucleotides has been studied extensively, only very little is known about the properties of PNA–dsDNA triplexes—mainly due to the competing invasion process. Here we show that when appropriately modified using pseudoisocytosine substitution, in combination with (oligo)lysine or 9-aminoacridine conjugation, homopyrimidine PNA oligomers bind complementary dsDNA targets via triplex formation with (sub)nanomolar affinities (at pH 7.2, 150 mM Na^+). Binding affinity can be modulated more than 1000-fold by changes in pH, PNA oligomer length, PNA net charge and/or by substitution of pseudoisocytosine for cytosine, and conjugation of the DNA intercalator 9-aminoacridine. Furthermore, 9-aminoacridine conjugation also strongly enhanced triplex invasion. Specificity for the fully matched target versus one containing single centrally located mismatches was more than 150-fold. Together the data support the use of homopyrimidine PNAs as efficient and sequence selective tools in triplex targeting strategies under physiological relevant conditions.

INTRODUCTION

Sequence-specific recognition of double-stranded (ds) DNA provides the fundamental basis for a vast repertoire of biological processes, and in chemical biology there is substantial progress towards development of synthetic ligands that emulate such recognition. Current strategies for sequence-selective dsDNA targeting include triplex forming oligonucleotides (TFOs) (1,2), synthetic hairpin polyamides (3), engineered zinc finger proteins (4–6) and peptide nucleic acids (PNAs) (7–9).

TFOs bind as a third strand in the major groove of dsDNA. In the classical 'pyrimidine motif', thymine/cytosine containing TFOs hybridize to the complementary adenine/guanine bases of the target in a parallel orientation via Hoogsteen base pairing (1). Conventional unmodified homopyrimidine TFOs exhibit relatively low target affinity at physiological pH. However, several modified TFOs such as those based on phosphoroamidate (10) and locked nucleic acid (LNA) (11) chemistries have been reported to exhibit improved triplex affinity.

The backbone of PNAs is composed of a charge neutral pseudopeptide (12) rather than the phospho-deoxyribose of DNA. Like homopyrimidine TFOs, homopyrimidine PNA oligomers bind complementary homopurine sequence targets in dsDNA. However, while homopyrimidine TFOs solely recognize dsDNA through major groove triplex formation, PNAs may bind dsDNA exploiting different predictable modes of recognition depending on the PNA and DNA sequence as well as ambient conditions. At high ionic strength and low concentrations of homopyrimidine PNA oligomer, conventional PNA–dsDNA Hoogsteen type triplexes are formed predominately in a parallel orientation (PNA amino terminal facing the 5′-end of the purine DNA strand), which judged by chemical probing share notable resemblance to ordinary TFO–dsDNA triplexes (13). At low ionic strength, high homopyrimidine PNA oligomer concentrations, or long reaction times, triplex invasion complexes dominate. These complexes are extremely stable (14) and contain an internal PNA–DNA–PNA triplex involving combined Hoogsteen (parallel orientation) and Watson–Crick (antiparallel orientation) base pairing and an unbound DNA strand displaced in a P-loop structure (15). For instance, a triplex invasion complex produced by a decamer thymidine PNA showed an extrapolated lifetime of several hundred days at 37°C and 140 mM Na^+ (16). Despite this very high stability and thus very low kinetic off-rates, triplex invasion complexes retain very high target selectivity through kinetic rather than thermodynamic

*To whom correspondence should be addressed. Tel: +45 35327762/61; Fax: +45 35396042; Email: ptrn@sund.ku.dk

The authors wish it to be known that, in their opinion, the first two authors should be regarded as joint First Authors.

© 2009 The Author(s)
This is an Open Access article distributed under the terms of the Creative Commons Attribution Non-Commercial License (http://creativecommons.org/licenses/by-nc/2.0/uk/) which permits unrestricted non-commercial use, distribution, and reproduction in any medium, provided the original work is properly cited.

discrimination (17). In essence, the specificity is controlled by differences in kinetic on-rates.

Mixed A–T/G–C dsDNA sequence targets can be recognized using pseudo-complementary (pc)PNAs in which diaminopurine (D) and thiouracil (U^S) substitute for adenine and thymine, respectively (18). A pair of pcPNAs bind complementary dsDNA targets *via* double duplex invasion through simultaneous formation of a D–T and U^S–A (and G–C or C–G) Watson-Crick base paired PNA–DNA helix with each of the complementary DNA strands. Complementary PNA–PNA Watson-Crick hybridization is strongly disfavored due to the D/U^S steric clash, but since no analogous G/C nucleobase substitutes are yet available, pcPNA sequence targets must contain a significant fraction ($\geq$50%) of A–T base pairs.

DsDNA containing mixed T–C stretches can be recognized via duplex invasion using sequence complementary homopurine PNA oligomers (19). Duplex invasion complexes involve an internal anti-parallel PNA–DNA hybrid with the non-complementary DNA strand being displaced. These complexes lack the stabilizing effect of a third strand seen upon triplex invasion (*vide supra*) and consequently are much less stable, but can form with PNAs that exhibit extraordinarily high stability of PNA–DNA duplexes such as seen for homopurine PNA (20). Furthermore, duplex invasion has been demonstrated using mixed sequence (conformationally constrained) gamma-PNAs conjugated to an acridine intercalator moiety (21). Helix invasion is very sensitive to even moderate concentrations of salt (14,22–27) through a very dramatic decrease in on-rate due to dsDNA duplex stabilization. PNA oligomers exhibiting very significantly enhanced dsDNA helix invasion binding can be obtained by conjugation to positively charged (e.g. lysine/arginine rich) peptides (28) or to the DNA intercalator 9-aminoacridine (29). Moreover, DNA supercoiling (22) and active transcription of a dsDNA template (26) strongly accelerate triplex invasion by homopyrimidine PNAs *in vitro* thereby suggesting that in live cells conditions may occur that support efficient helix invasion. To this end, unmodified mixed pyrimidine/purine sequence nonadecamer PNA oligomers used to target the two human progesterone promoter isoforms hPR-A and hPR-B in cell culture showed efficient and reagent sequence selective knock-down of progesterone receptor mRNA and protein using only 12–50 nM PNA oligomer (30). Importantly, since the PNAs used were complementary to the DNA template strand—and not the RNA—the results were compatible with a DNA level mechanism, possibly by targeting of the RNA polymerase–dsDNA open complex (30) as previously reported for DNA oligonucleotides using an *E. coli* RNA polymerase *in vitro* system (31).

Because unmodified mixed sequence purine/pyrimidine PNAs do not bind efficiently to naked dsDNA *via* helix invasion, this suggests that the cellular environment may significantly alter target accessibility. Nonetheless, helix invasion remains much more sensitive to increased ionic strength conditions as compared with triplex formation, and while known for several years (32), only more recently has it become clear that PNA–dsDNA triplexes can be stably formed when using dodecamer and pentadecamer homopyrimidine PNAs (13,33). Thus homopyrimidine based PNA–dsDNA triplexes could present significant advantages over helix invasion approaches under physiological conditions. Consequently, we have now in more detail studied the requirements for and effects of chemical modifications on PNA–dsDNA triplex formation, including parameters that determine the distribution of triplex versus invasion type complexes at physiologically relevant ionic strength conditions.

EXPERIMENTAL

PNA oligomers

PNA oligomers (Table 1) were synthesized as described (34), purified by reversed phase HPLC and characterized by Maldi-TOF mass spectrometry (Table S1).

DNA constructs

Plasmid constructs used in this study (Table 1, see Tables S2 and S3 for construction details) were derived from p322 (13), using standard methodology (35), propagated in *E. coli* strain DH5α, and purified by maxipreparation (Jet Star).

Preparation of ^{32}P-labeled dsDNA targets

The relevant dsDNA plasmid was *Pvu*II–*Xba*I restriction digested (or *Eco*RI–*Pvu*II restriction digested for preparation of ^{32}P-DNA for DMS probing, Supplementary Data), followed by phenol extraction and precipitation using 2% potassium acetate in 96% ethanol. The DNA was resuspended in H_2O and ~10 μg was used for isotope labeling using the Klenow fragment of DNA polymerase I, [α^{-32}P]dATP and unlabeled dCTP, dGTP and dTTP as recommended (Invitrogen). The samples were resolved by 5% native TBE buffered polyacrylamide gel-electrophoresis (30:1 in acrylamide to bisacrylamide), and the 172 bp fragment carrying the relevant PNA sequence target was identified by autoradiography and excised followed by elution from gel slices over night in 0.5 M NH_4-acetate, 1 mM EDTA [when derived from p322, the 172 bp fragment is identical with that used in Bentin *et al.* (13), but which was previously identified as 168 bp due the inadvertent omission of the four nucleotides of the *Xba*I derived overhang]. ^{32}P-end labeled DNA was ethanol precipitated, washed once with 70% ethanol, air-dried, and resuspended in 50 μl 10 mM sodium phosphate pH 7 on ice and stored at –20°C.

Gel-shift analysis

Gel-shift analyses were carried out using an estimated amount of ^{32}P-DNA of ~2 nM and 0–4.5 μM PNA in a buffer containing 150 mM sodium, 10 mM phosphate and 0.5 mM EDTA and adjusted to the indicated pH in a final volume of 30 μl at 37°C over night or for the indicated length of time. Subsequently, the samples were supplemented with 5 μl 5 × TAE loading buffer and 5 μl/well was analyzed using a Life Technologies model S2 gel apparatus and native TAE buffered 10% polyacrylamide

gels (30% acrylamide: 1% *bis*-acrylamide) run at 500 V for 16–20 h at 4°C. Gelshift analysis of LNA1 binding to dsDNA (Supplementary Data) was as for PNA but using a V15-17 apparatus (Life Technologies) with 20 µl sample/well and run at 300 V, 2.5 h at 4°C. The gels were vacuum-dried and analyzed by phosphor imaging and the data was processed using Image Quant software.

DNaseI footprinting

Samples for *DNase*I footprinting (Figure 1) were similar to those for gel-shift analysis using an estimated amount of ^{32}P-DNA of ~2 nM and 0–4.5 µM PNA1846 or 0–40.5 µM TFO1 at pH 6.3 and supplemented with 1.5 mM $MgCl_2$ (i.e. 1 mM effective magnesium) to enhance binding of the TFO in a final volume of 60 µl and incubation was 1 h 37°C. A *DNase*I titration was first conducted using naked DNA to establish the optimal enzyme concentration under the given conditions (data not shown). Based on this, footprinting was conducted by supplementing the above PNA–dsDNA incubations with 33 pg *DNase*I (Sigma) in a buffer containing 2 mM $MgCl_2$, 1 mM $CaCl_2$ and 1 mM NaCl at a final volume of 100 µl for 5 min at room temperature. The reactions were stopped by addition of 3 µl 0.5 M EDTA and ethanol precipitated. The supernatants were discarded and the pellets air-dried and resuspended in 10 µl formamide loading buffer, heated to 90°C for 2 min and immediately placed on ice. Samples (5 µl/well) were resolved using a Life Technologies model S2 gel apparatus and 10% TBE buffered polyacrylamide gels (30:1 in polyacrylamide to bisacrylamide) containing 7 M urea and visualized by autoradiography.

Table 1. PNA and DNA sequences used in this study

PNA	
84	H-TTTTTCTCTCTCTCT-NH_2
1846	H-TTTTTCTCTCTCTCT-Lys-NH_2
2998	H-CTCTCTCTCT-Lys-NH_2
2999	H-TCTCTCTCTCT-Lys-NH_2
3000	H-TTCTCTCTCTCT-Lys-NH_2
3001	H-TTTCTCTCTCTCT-Lys-NH_2
3002	H-TTTTCTCTCTCTCT-Lys-NH_2
3003	Acr-eg1-TTTTTCTCTCTCTCT-Lys-NH_2
3004	Acr-Acr*-eg1-TTTTTCTCTCTCTCT-Lys-NH_2
3005	H-Lys-TTTTTCTCTCTCTCT-Lys-NH_2
3006	H-$(Lys)_2$-TTTTTCTCTCTCTCT-Lys-NH_2
3007	H-$(Lys)_3$-TTTTTCTCTCTCTCT-Lys-NH_2
3015	H-TTTTTJTJTJTJTJT-Lys-NH_2
3049	Acr-eg1-TTTTTJTJTJTJTJT-Lys-NH_2
3050	Acr-Acr*-eg1-TTTTTJTJTJTJTJT-Lys-NH_2
3051	H-$(Lys)_3$-TTTTTJTJTJTJTJT-Lys-NH_2
3095	H-$(Lys)_3$-TTTTJTJTJT-Lys-NH_2
3096	Acr-eg1-TTTTJTJTJT-Lys-NH_2
3097	Acr-Acr*-TTTTJTJTJT-Lys-NH_2
DNA	
TFO1	5′-d(TTTTTCTCTCTCTCT)-3′
p322	5′... d(TAT**AAAAAGAGAGAGAGA**TCG) ...3′
p395	5′... d(TAT**AAAAAGATAGAGAGA**TCG) ...3′
p396	5′... d(TAT**AAAAAGAAAGAGAGA**TCG) ...3′
p397	5′... d(TAT**AAAAAGACAGAGAGA**TCG) ...3′

Upper panel: PNAs used in the present study (written from the N→C terminus). Thymine (T), cytosine (C), pseudoisocytosine (J), *N*-(acridin-9-yl)-6-aminohexanoic acid (Acr), *N*-(acridin-9-yl)-6-aminohexanoylaminoethyl glycine ('acridine-aeg')(Acr*) (41), lysine (Lys), ethylene glycol (eg1). *Lower*: Sequence of the oligonucleotide TFO1 and plasmid PNA targets (only the purine strand is shown). Bold letters indicate PNA target, underlined letters indicate positions mismatched relative to the PNAs.

RESULTS

Design of PNA oligomers

Previous results have shown that stable non-invasion PNA–dsDNA triplexes can be formed using dodecamer and pentadecamer homopyrimidine PNA oligomers whereas a decamer homopyrimidine PNA was too short as investigated using gel-shift analysis. However, when probed directly in solution using dimethyl sulphate, triplex formation was detected even for decamers (13). Consequently, PNA oligomers in the range decamer to pentadecamer were chosen for evaluation in the present study (Table 1).

PNA versus TFO containing triplexes

In order to investigate the target binding efficiency of PNA relative to a triplex forming oligo-deoxyribonucleotide and thus set the framework for the utility of PNA oligomers in triplex strategies, the binding of a pentadecamer homopyrimidine PNA (PNA1846) and a TFO (TFO1) of identical sequence (Table 1) was analyzed in parallel by *DNase*I footprinting (Figure 1). Triplex formation by TFOs containing cytosine is highly pH dependent due to the requirement for protonation at cytosine N3. Consequently, the experiments were conducted at slightly acidic pH (pH 6.3). To enhance binding of the TFO further, magnesium was included to shield phosphate backbone repulsion. Finally, all experiments were performed at 0.15 M monovalent salt because our aim was to compare binding at physiologically relevant ionic strength conditions. Both oligomers show target specific footprints (Figure 1A) with half target protection at ~16 nM and ~3.4 µM for PNA1846 and TFO1, respectively (Figure 1B). Thus PNA1846 binding is superior by more than 200-fold compared to TFO1 as investigated by footprinting analysis.

Because triplex formation and triplex invasion cannot be distinguished by *DNase*I footprinting (yielding similar footprints), gel-shift analysis was employed. Band assignments were according to our previous report (13), and as further described in the Figures S1 and S2. To qualify the approach, we first measured the binding efficiency of PNA1846 for triplex binding to its dsDNA target and obtained an EC_{50} value (vide infra) of ~17 nM at pH 6.3 (Figure 1C and D, Table 2). Thus, *DNase*I footprinting and gel-shift analysis produced quantitatively similar results. Consistent with previous observations (13), the triplex shifted to triplex invasion complexes thereby reducing the absolute amount of triplex when the PNA concentration was increased (Figure 1D).

To evaluate whether PNA1846–dsDNA triplex formation was at equilibrium, we performed an off-rate measurement by gel-shift analysis. This yielded a triplex half-life of ~6 h at 37°C confirming that over-night

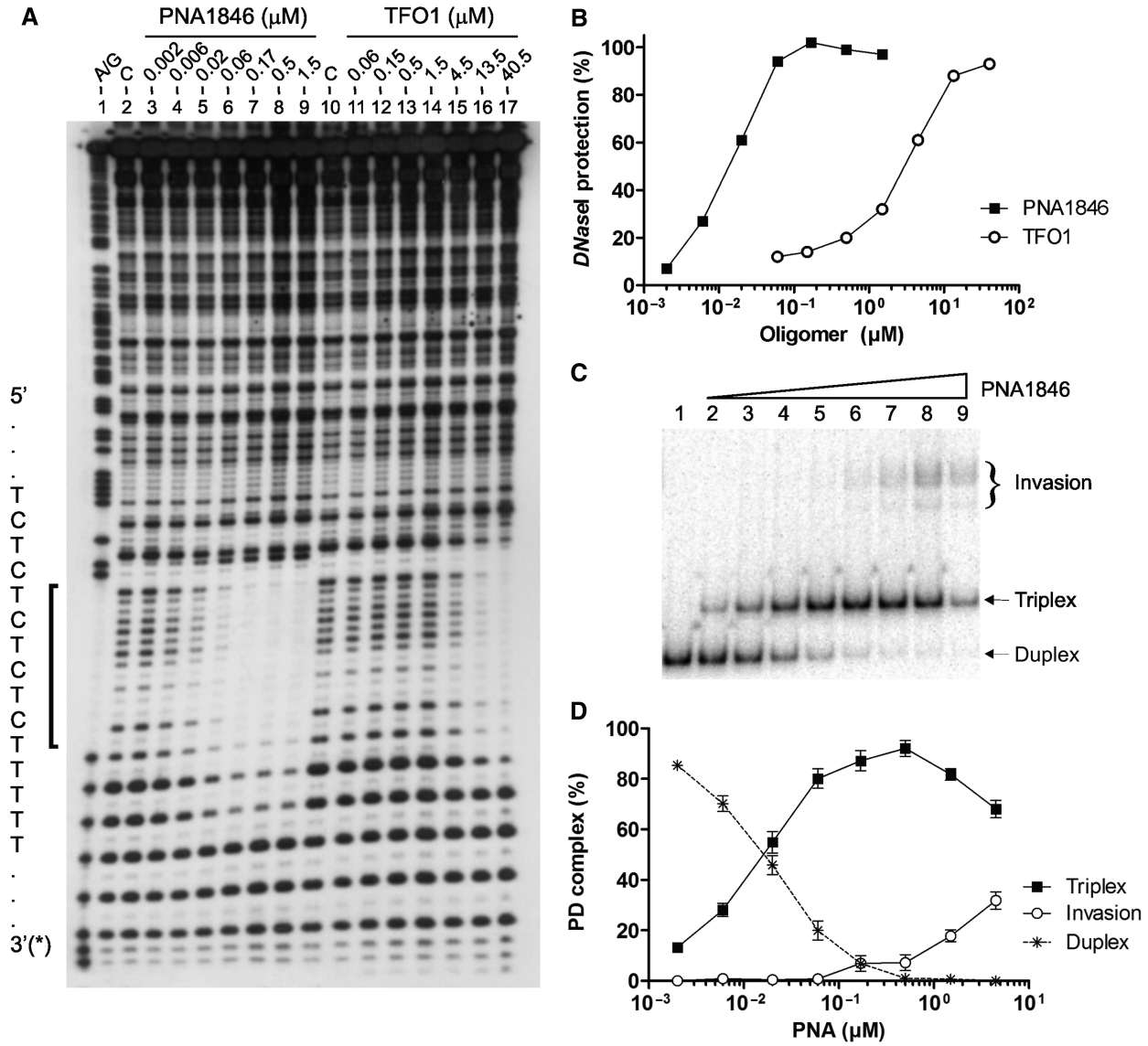

Figure 1. Comparison of PNA oligomer and TFO binding to the complementary dsDNA target at pH 6.3. (**A**) Autoradiograph showing *DNase* I footprint formed by PNA1846 (lanes 3–9) and TFO1 (lanes 11–17) bound to the complementary dsDNA target from p322. The position of the sequence target is indicated adjacent to the A/G sequence reaction (lane 1). Asterisk indicates the position of the ^{32}P-label. Lanes 2 and 10 are controls without oligomer. (**B**) Quantitative analysis of the data shown in (A). Percentage *DNase*I protection as a function of PNA1846 or TFO1 concentration. (**C**) Autoradiograph showing PNA1846 binding to the complementary sequence target in p322 as analysed by gel-shift analysis. The following PNA1846 concentrations (μM) were used: w/o (lane 1), 0.002 (lane 2), 0.006 (lane 3), 0.02 (lane 4), 0.06 (lane 5), 0.17 (lane 6), 0.5 (lane 7), 1.5 (lane 8) and 4.5 (lane 9). (**D**) Percentage PD-complex (triplex or invasion) formed as a function of PNA concentration is shown. Free dsDNA is included for reference (indicated as duplex). Error bars indicate standard error of the mean (SEM) of six experimental repetitions. Notice the bell-shaped curve for triplex formation. Also notice the logarithmic scale of the *x*-axis.

incubations would have produced a PNA1846 triplex system at equilibrium (data not shown). This is in stark contrast to the situation observed for triplex invasion, which is kinetically controlled even when using homopyrimidine PNA oligomers of only 10 bases (17). However, because we did not do the analysis for the entire set of PNAs, we cannot formally rule out the possibility that triplex formation by some of the more strongly binding PNAs has not reached equilibrium during the experiment. Moreover, the better performing PNAs showed efficient target occupancy at concentrations approaching that of the DNA concentration, under which circumstances the conditions for pseudo-first order kinetics are no longer upheld. Finally, due to the variable propensity for conversion of triplex to triplex invasion complex, it is not possible to treat these species as independent, and given their different stability we do not assign true K_d values. Consequently, we report the data as EC_{50} values (i.e. the amount of PNA oligomer that yields 50% DNA binding under the given conditions) and not as equilibrium constants. At worst, this approach would give an underestimate of the true K_d values.

Table 2. EC_{50} values for PNA binding to a fully matched dsDNA target[a]

PNA	Length	c/m/b	pH	EC_{50}
2999	11	+2/-/C	6.3	>4.5 μM
3000	12	+2/-/C	6.3	0.4 μM
3001	13	+2/-/C	6.3	0.15 μM
3002	14	+2/-/C	6.3	50 nM
1846	15	+2/-/C	6.3	17 nM
1846	15	+2/-/C	5.5	<2 nM
1846	15	+2/-/C	6.7	0.45 μM
1846	15	+2/-/C	7.2	2.2 μM
1846	15	+2/-/C	7.7	3.2 μM
1846	15	+2/-/C	8.2	3.5 μM
84	15	+1/-/C	6.3	14 nM
3005	15	+3/-/C	6.3	8 nM
3006	15	+4/-/C	6.3	<2 nM
3007	15	+5/-/C	6.3	<2 nM
3007	15	+5/-/C	7.2	0.16 μM
3003	15	+2/Acr/C	7.2	80 nM (0.53 μM)
3004	15	+3/Acr_2/C	7.2	<2 nM (4 nM)
3015	15	+2/-/J	7.2	0.15 μM
3051	15	+5/-/J	7.2	7 nM
3049	15	+2/Acr/J	7.2	<2 nM (0.18 μM)
3050	15	+3/Acr_2/J	7.2	<2 nM (10 nM)

[a]EC_{50} values for the indicated PNAs and at the given pH upon binding to the complementary dsDNA target from p322. When relevant, EC_{50} values for triplex invasion are given in brackets. In column 3, c/m/b indicates the PNA net charge, terminal modification and whether it contains C- or J-nucleobases (see Table 1). The EC_{50} values were determined manually using the graphs in Figures 1–7 and 9).

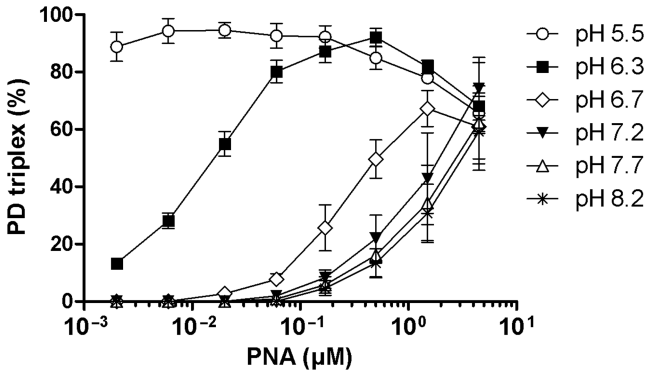

Figure 2. Effect of pH on pentadecamer PNA-dsDNA triplex formation. The graph shows percentage PD triplex formed at the indicated pH as a function of the PNA1846 concentration upon binding to the complementary dsDNA sequence target as determined by gel-shift analysis. Error bars indicate SEM using three to four experimental repetitions, except for the data from pH 6.3 where the data from Figure 1C is included for reference. See Figure S3 for example of gel-shift data.

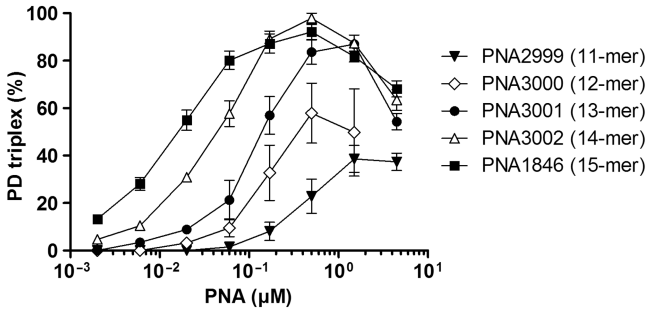

Figure 3. Effect of PNA length on PNA-dsDNA triplex formation at pH 6.3. The graph shows percentage PD triplex formed as a function of the PNA concentration upon binding to the complementary dsDNA target as determined by gel-shift analysis and using the indicated (+2) PNA oligomers. Error bars indicate SEM using two to three experimental repetitions, except for the data from pH 6.3 where the data from Figure 1C is included for reference. See Figure S4 for example of gel-shift data.

pH dependency

To evaluate the pH dependency on triplex recognition gel-shift experiments were conducted in the pH range 5.5–8.2 (Figure 2, Table 2). As expected, increasing the pH reduced binding of PNA1846 thus increasing EC_{50} from <2 nM at pH 5.5 to ~2.2 μM at 7.2. Above pH 7.2, any further decrease of binding was limited yielding EC_{50} values of ~3.2 and ~3.5 μM at pH 7.7 and 8.2, respectively, which suggests that most cytosine N3 residues were fully non-protonated at this pH. This extremely steep correlation between the efficiency of triplex formation and the pH, from and below pH 7.2, mirrors that expected for TFO–dsDNA Hoogsteen base pairing. At pH 5.5, the triplex was almost fully formed even at the lowest PNA concentration (2 nM).

Effects of PNA length

Truncation from the N-terminus of PNA1846 by one base at a time resulted in a shift of the binding isotherm at pH 6.3 towards higher PNA concentration. For the PNA pentadecamer–dodecamer oligomers (PNAs 1846, 3002, 3001, 3000), a 2–3-fold reduction of binding efficiency was observed per nucleobase deleted yielding EC_{50} values ranging from ~17 nM to ~0.4 μM (Figure 3, Table 2). Binding of the undecamer PNA2999 was further reduced more than 10-fold as compared with dodecamer PNA3000 (Table 2). In accordance with previous results (13), no triplex binding was detected by gel-shift analysis using the decamer PNA (data not shown). Thus an unmodified undecamer PNA of the given composition is the shortest PNA that yield triplex binding detectable by gel-shift analysis.

Effects of PNA net charge

As observed for helix invasion (22,29), introduction of up to five positive charges strongly enhanced PNA–dsDNA triplex binding at pH 6.3 to an extent where the PNA oligomer titration approached stoichiometric binding to the dsDNA target (Figure 4, Table 2). For instance, the EC_{50} of pentadecamer PNAs containing a net charge of +4 (PNA3006) and +5 (PNA3007) were <2 nM and thus could not be accurately determined in the assay at pH 6.3. Consequently, we changed to a physiologically relevant pH (7.2). At this pH, which in terms of triplex formation is highly unfavorable, EC_{50} values of ~0.16 and ~2.2 μM were obtained for the +5 PNA3007 and +2 control PNA1846 PNA oligomers, respectively (Figure 5, Table 2). Thus a ~14-fold improvement in triplex

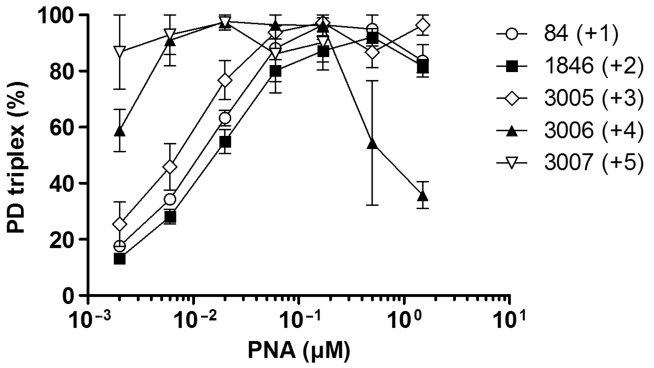

Figure 4. Effect of PNA net-charge on pentadecamer PNA–dsDNA triplex formation at pH 6.3. The graph shows percentage PD triplex formed as a function of the concentration of the (+1 to +5) PNA oligomers upon binding to the complementary dsDNA sequence as determined by gel-shift analysis using the indicated PNA oligomers. Error bars indicate SEM using two experimental repetitions, except for the data from pH 6.3 where the data from Figure 1C is included for reference. See Figures S5 and S3 for example of gel-shift data.

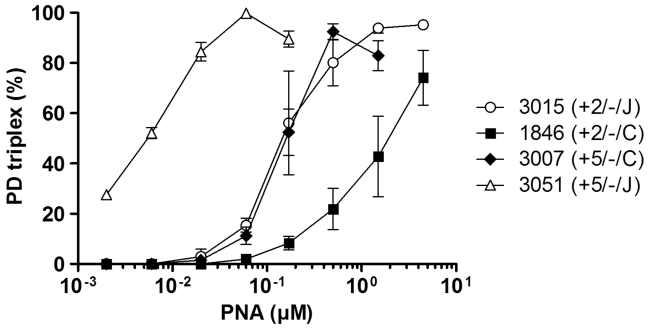

Figure 5. Triplex formation by J-base versus cytosine containing pentadecamer PNAs at pH 7.2. The graph shows percentage PD triplex formed as a function of the PNA concentration on binding to the complementary dsDNA target using the indicated PNA oligomers. The symbol nomenclature is similar to that given in Table 2, column 3. Error bars indicate SEM using two to three experimental repetitions. See Figures S6 and S3 for example of gel-shift data.

formation is achieved by introduction of three additional positive charges.

J-base modified PNAs

With the expectation to eliminate or at least dramatically reduce the pH dependency of triplex formation, we investigated the effect of substituting pseudoisocytosine (J) for cytosine (36). At pH 7.2, a J-base containing PNA pentadecamer carrying a net charge of +2 (PNA3015) or +5 (PNA3051) showed EC_{50} values of ~0.15 and ~7 nM, respectively, as compared to the EC_{50} values for the corresponding cytosine PNAs of ~2.2 (PNA1846) and ~0.16 μM (PNA3007) (Figure 5, Table 2). Thus J-base substitution yields PNA oligomers with ~15- (+2) and ~23-fold (+5) improved triplex binding relative to that of the corresponding cytosine PNAs. Consistent with previous results (36), these data show that J-base substitution

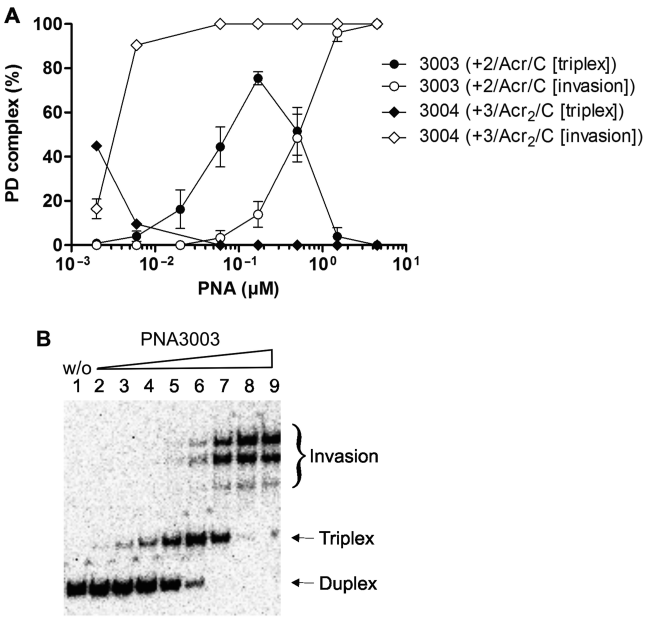

Figure 6. Triplex formation and triplex invasion by 9-aminoacridine modified pentadecamer PNAs at pH 7.2. (**A**) Graph showing percentage PD complex (triplex or invasion) formed as a function of the PNA concentration on binding to the complementary sequence target in p322. (**B**) Autoradiograph showing an example of gel-shift analysis of PNA3003 binding to dsDNA. The following PNA oligomer concentrations (μM) were used: w/o (lane 1), 0.002 (lane 2), 0.006 (lane 3), 0.02 (lane 4), 0.06 (lane 5), 0.17 (lane 6), 0.5 (lane 7), 1.5 (lane 8) and 4.5 (lane 9). The symbol nomenclature is similar to that given in Table 2, column 3. Error bars indicate SEM using two to three experimental repetitions.

almost fully eliminates the pH sensitivity of Hoogsteen binding.

9-Aminoacridine modified PNAs

9-Aminoacridine modification of PNA is known to strongly enhance triplex invasion for both mono- and bis-PNA (29). Consequently, we decided to investigate the effect of 9-aminoacridine conjugation on Hoogsteen type PNA–dsDNA triplex formation at pH 7.2 (Figure 6, Table 2). The introduction of a single 9-aminoacridine moiety into the cytosine containing PNA1846 yielded PNA3003 (+2), which exhibited an EC_{50} value for triplex formation of ~80 nM as compared with ~2.2 μM for the unmodified PNA1846 corresponding to a ~28-fold enhancement. PNA3003 also showed an enhanced propensity for strand invasion (with an EC_{50} of ~0.53 μM) thus making triplex and triplex invasion complexes difficult to completely separate by titration.

The double 9-aminoacridine modification of cytosine-containing PNA3004 (+3) improved binding even further at pH 7.2 (Figure 6). The EC_{50} value for triplex formation exceeded what could be measured (i.e. <2 nM) and the propensity for strand invasion was even further increased showing an EC_{50} of ~4 nM. It should be noted that double 9-aminoacridine modification inherently also contributes an additional charge to PNA3004 (Table 1). Therefore, the enhanced binding relative to PNA3003

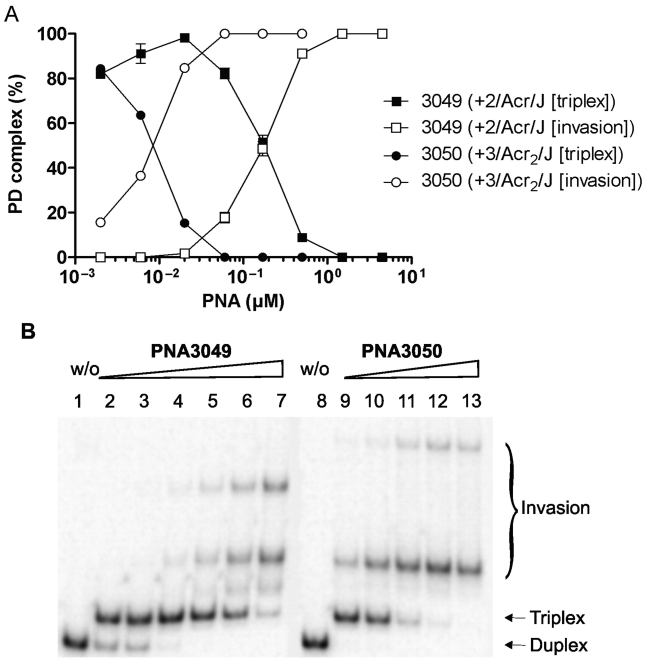

Figure 7. Triplex formation and triplex invasion by 9-aminoacridine modified J-base pentadecamer PNAs at pH 7.2. (**A**) The graph shows percentage PD complex (triplex or triplex invasion as specified in the symbol explanation) formed as a function of the PNA concentration using the indicated PNA oligomer and the complementary dsDNA sequence target. The symbol nomenclature is similar to that given in Table 2, column 3. (**B**) Autoradiograph showing an example of a gel-shift experiment using PNAs 3049 and 3050 at the following (μM) concentrations: w/o (lanes 1 and 8), 0.002 (lanes 2 and 9), 0.006 (lanes 3 and 10), 0.02 (lanes 4 and 11), 0.06 (lanes 5 and 12), 0.17 (lanes 6 and 13) and 0.5 (lane 7).

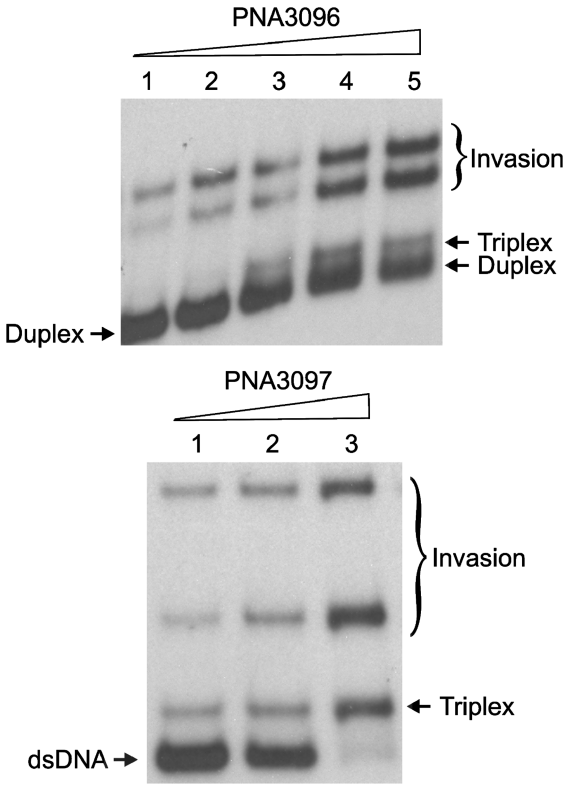

Figure 8. Triplex formation and triplex invasion by 9-aminoacridine and J-base modified decamer PNAs at pH 7.2. Autoradiographs showing gel-shift analysis of the binding of the indicated PNAs to the complementary target in p322. PNA–dsDNA binding was for 2 h (to favor triplex formation over helix invasion) and as stated in the experimental except that 2.5 mM $MgCl_2$ (2 mM effective concentration) was included. The following PNA concentrations (μM) were used: lane 1 (0.06), lane 2 (0.17), lane 3 (0.5), lane 4 (1.5) and lane 5 (4.5).

resulted from a combination of the extra intercalator and added charge.

9-Aminoacridine and J-base modified PNAs

Considering the above results, it is of no surprise that combination of the J-base and acridine modifications (PNA3049 and PNA3050) improved binding even further. Indeed, virtually full triplex formation was seen even at the lowest PNA concentrations used, i.e. both give EC_{50} values $\ll$2 nM even at pH 7.2 (Figure 7, Table 2). Similarly to the results obtained with acridine modified cytosine PNA (Figure 6), such 9-aminoacridine/J-base containing PNA oligomers show a strong propensity for triplex invasion (EC_{50} values of $\sim$0.18 μM and $\sim$10 nM for singly (PNA3049) and doubly (PNA3050) acridine modified PNAs, respectively). Notably, as compared with doubly acridine modified PNA3050 (Figure 7B), the J-base modification alone (PNA3051, Figure S6), more selectively allows for triplex only binding.

9-Aminoacridine modified decamer PNAs

The cytosine containing decamer PNA2998 did not show detectable binding in the gel-shift assay (data not shown). Given the significant enhancement of the EC_{50} values obtained by J-base substitution and 9-aminoacridine modification of a pentadecamer PNA oligomer, we decided to investigate whether such modification of the decamer PNA would support triplex recognition. No significant binding could be detected using the +5 J-base modified decamer PNA3095 at 4.5 μM (data not shown). In contrast, singly (+2) and doubly (+3) 9-aminoacridine modified PNA3096 and PNA3097 did indeed show triplex binding by gel-shift analysis (Figure 8). Notably, however, only limited triplex formation was observed since binding occurred predominately via triplex invasion, consistent with the observation that intercalator modification enhances PNA triplex invasion at elevated ionic strength conditions (29). Moreover, these binding modes could not be uncoupled, neither by altering the PNA concentration (Figure 8), nor by changing the length of incubation (data not shown). Thus triplex recognition is not sufficiently stabilized by charge or by combined acridine/J-base modification, but requires extended PNA oligomers.

Theoretically, triplex binding should follow pseudo-first order kinetics, whereas triplex invasion requiring two PNA strands should follow pseudo-second order kinetics [in fact experimental data have suggested more complex kinetics yielding a slightly higher reaction order for triplex invasion (17)]. Therefore, the ratio between the velocity for triplex invasion (v_{TI}) and triplex formation

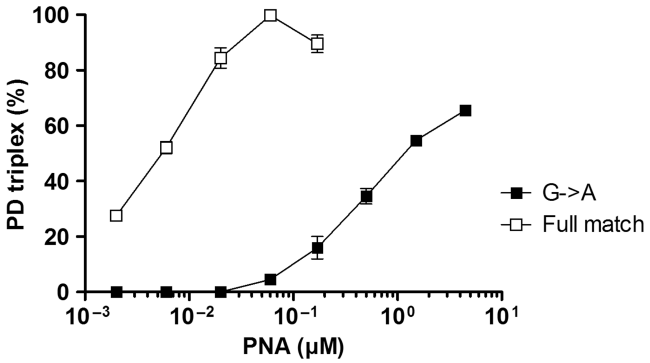

Figure 9. Specificity of J-base modified pentadecamer triplex formation at pH 7.2. The graph shows percentage triplex formed as a function of the (+5) PNA3051 concentration with dsDNA containing a fully matched target (data from Figure 5 is included for reference) or a singly G–C→ A–T mismatched target (indicated as G→A in the figure). Error bars indicate SEM using two experimental repetitions. See Figures S7 and S6 for example of gel-shift data.

(v_T) complexes $v_{TI}/v_T = k_{TI}[PNA]^2/k_T[PNA]$ (where k_{TI} and k_T are the rate constants for triplex invasion and triplex formation, respectively), will increase with increasing PNA concentration following the kinetic characteristics of the two binding curves. Consequently, PNA oligomers having low affinity for triplex binding will, in general, show a relatively higher propensity for triplex invasion binding. This property is clearly exemplified by decamer PNA3096, because the required PNA concentration is so high that triplex invasion complexes become preferred (Figure 8). Finally, the relative (and absolute) amount of triplex invasion product will increase with increasing incubation time (as triplex invasion is fully kinetically controlled), and will decrease with increasing cation [in particular di- (e.g. Mg^{2+}) and multivalent (e.g. spermine) cation] concentration as the DNA double helix is stabilized.

Target selectivity

The utility of PNA–dsDNA triplexes for sequence specific dsDNA targeting also relies on the sequence selectivity of the interaction. To investigate this parameter, we prepared three new dsDNA fragments each containing a single G–C → A–T, G–C → T–A or G–C → C–G alteration centrally located within the PNA target sequence (Table 1) and challenged these constructs with the reference PNA1846. Because this PNA performs relatively poorly at pH 7.2 ($EC_{50} \sim 2.2\,\mu M$), we used pH 6.3 ($EC_{50} \sim 17\,nM$). In spite of this, no significant triplex formation was detected with any of the singly mismatched constructs (data not shown). Because one main aim was to clarify the binding properties under physiologically relevant conditions, we further investigated the target selectivity of one of the best performing PNAs at pH 7.2. PNA3051 combines a high dsDNA affinity and efficient triplex binding making this PNA oligomer an obvious choice for that purpose (see Figure S6). When challenging this PNA with the fully complementary target producing J–G–C base triplets (where J is PNA pseudoisocytosine) versus a DNA fragment containing a single central J–A–T mismatch, EC_{50} values of ~7 nM and ~1.25 μM were obtained (Figure 9). Importantly, no significant binding was detected with either of the singly mismatched J–T–A, or J–C–G targets (data not shown). Consequently, PNA3051 shows more than 150-fold preference for the fully matched target over any of the singly centrally positioned mismatched targets employed.

DISCUSSION

The present data very clearly demonstrate that the ratio of triplex binding versus triplex invasion is critically dependent on PNA concentration, oligomer length, and composition (as well as reaction time). Triplexes are increasingly stabilized in the range undecamer–pentadecamer consistent with previous observations (13). As expected, J-base modification, which allows the oligomer to function both in a G–C Watson–Crick binding mode as well as in a CG–C+ Hoogsteen binding mode due to the tautomeric equilibrium of the nucleobase (36), significantly decreases the pH dependency (sensitivity) on triplex recognition, and additional positive charges (in the form of conjugated lysines), and acridine modification significantly enhances triplex affinity. However, acridine conjugation also significantly accelerates helix invasion at the expense of triplex formation.

In assessing the general utility of modified PNA oligomers as triplex targeting agents, comparison to published TFO chemistries is relevant. Obviously such comparison is complicated by the different sequences, hybridization conditions and methods of analysis employed by different groups and consequently no direct side by side comparison is possible in a meta analysis. Nevertheless, a comparison based on available data for some of the most promising TFOs–LNAs and phosphoroamidites, is informative. A study of LNA mix-mers conjugated to 2-methoxy-6-chloro-9-aminoacridine, revealed a 5–10 nM EC_{50} value for binding of the hexadecamer 5′-tTtTcTtTtCcCcCct-3′ (where lower case letters represent the LNA ribonucleotides containing the 2′-O, 4′-C methylene linkage, capital letters represent standard deoxyribonucleotides, and all cytosines are methylated in position 5) to its complementary target at pH 7.2 (37). Several pentadecameric PNAs in the present study show low nanomolar (e.g. PNA3051) or sub-nanomolar (PNA3049 and PNA3050) EC_{50} values for triplex formation at pH 7.2, which rivals or indeed supersedes the dsDNA triplex affinity of reported acridine conjugated hexadecameric LNA oligomers. In order to make a more direct comparison of PNA versus LNA, the binding of LNA1 (which is sequence identical to the pentadecamer PNAs used in the present study, but containing 5-methylcytosine) to its complementary target was studied (Figure S8). While no significant binding was detected at pH 7.2 (data not shown), a gel-shifted band was seen at low nanomolar LNA1 concentrations at pH 6.3 (Figure S8) (this is consistent with triplex recognition). However, binding reached substantially <50% target saturation, and curiously the band shift disappeared at higher LNA

concentrations. We have presently no explanation for these observations but speculate that higher order LNA1 complexes could contribute.

Phosphoramidates (linked by N3′–P5′ phosphoramidate bonds), form thymine–cytosine pyrimidine motif triplex structures that are thermally stabilized relative to isosequential phosphodiester containing oligonucleotides (38). The triplex melting temperature at pH 7.0 of a hexadecamer homopyrimidine phosphoramidate with the sequence 5′-TTTTCTTTTCCCCCCT-3′ was 40°C as compared with <10°C for unmodified oligonucleotide, and from the published restriction enzyme cleavage inhibition data (39) we estimate the corresponding EC_{50} value for binding to plasmid DNA as ~0.2 μM [Figure 2 (39)]. The +5 cytosine PNA3007 binds with a comparable EC_{50} value of ~0.16 μM at pH 7.2. While substituting 5-methyl cytosine for cytosine further improved both the thermal stability (T_m = 47°C) and the triplex EC_{50} of the hexadecameric phosphoramidate (>90% saturation at 0.2 μM) (39), pentadecameric homopyrimidine J-base substituted PNA3051 show much enhanced triplex binding (EC_{50} ~ 7 nM).

Thus, in terms of binding efficiency, homopyrimidine PNA oligomers clearly match or exceed that of similar LNA or phosphoramidate constructs. However, the present PNA oligomers also show a variable propensity for strand invasion that must be taken into account during experimental designs. The present results also have implications concerning possible *in vivo* gene targeting using PNA. In contrast to dsDNA targeting via [triplex or (double) duplex] invasion mechanisms, PNA triplex binding is not adversely affected by physiological ionic strength conditions. Thus PNA triplex recognition of accessible dsDNA targets is expected to readily take place in cells *in vivo*. Furthermore, PNA triplex formation also much less dramatically changes the DNA structure as compared to P-loop formation, and therefore the modulation effects on DNA metabolism, such as transcription, replication, recombination and repair processes will be different. Therefore despite of the general restrictions of sequence targets (homopurine), PNA triplex targeting should significantly expand the *in vivo* potential of PNA oligomers.

Finally, we note that synthetic bases for triplex recognition of purine–pyrimidine mixed sequence targets as developed in an oligonucleotide context (40) might be exploited with PNA, thereby increasing the sequence repertoire for PNA–dsDNA triple helix formation. Therefore, well designed triplex forming PNA oligomers expend the repertoire of effective sequence selective dsDNA targeting modalities.

SUPPLEMENTARY DATA

Supplementary Data are available at NAR Online.

FUNDING

European Commission (6th FP project SNIPER contract no. LSHB-CT-2004-005204) (PEN), the Novo Nordic Foundation (TB/MEH) and The Danish Medical Research Council (PEN/TB). Funding for open access charge: University of Copenhagen.

Conflict of interest statement. None declared.

REFERENCES

1. Chin,J.Y., Schleifman,E.B. and Glazer,P.M. (2007) Repair and recombination induced by triple helix DNA. *Front Biosci.*, **12**, 4288–4297.
2. Rogers,F.A., Lloyd,J.A. and Glazer,P.M. (2005) Triplex-forming oligonucleotides as potential tools for modulation of gene expression. *Curr. Med. Chem. Anticancer Agents*, **5**, 319–326.
3. Dervan,P.B., Doss,R.M. and Marques,M.A. (2005) Programmable DNA binding oligomers for control of transcription. *Curr. Med. Chem. Anticancer Agents*, **5**, 373–387.
4. Porteus,M.H. and Carroll,D. (2005) Gene targeting using zinc finger nucleases. *Nat. Biotechnol.*, **23**, 967–973.
5. Durai,S., Mani,M., Kandavelou,K., Wu,J., Porteus,M.H. and Chandrasegaran,S. (2005) Zinc finger nucleases: custom-designed molecular scissors for genome engineering of plant and mammalian cells. *Nucleic Acids Res.*, **33**, 5978–5990.
6. Carroll,D. (2008) Progress and prospects: zinc-finger nucleases as gene therapy agents. *Gene Ther.*, **15**, 1463–1468.
7. Bentin,T., Larsen,H.J. and Nielsen,P.E. (2004) Peptide nucleic acid targeting of double-stranded DNA. In Nielsen,P.E. (ed.), *Peptide Nucleic Acids: Protocols and Applications*. Horizon Bioscience, Wymondham, Norfolk, pp. 107–140.
8. Kaihatsu,K., Janowski,B.A. and Corey,D.R. (2004) Recognition of chromosomal DNA by PNAs. *Chem. Biol.*, **11**, 749–758.
9. Lundin,K.E., Good,L., Stromberg,R., Graslund,A. and Smith,C.I. (2006) Biological activity and biotechnological aspects of peptide nucleic acid. *Adv. Genet.*, **56**, 1–51.
10. Besch,R., Giovannangeli,C. and Degitz,K. (2004) Triplex-forming oligonucleotides—sequence-specific DNA ligands as tools for gene inhibition and for modulation of DNA-associated functions. *Curr. Drug Targets*, **5**, 691–703.
11. Vester,B. and Wengel,J. (2004) LNA (locked nucleic acid): high-affinity targeting of complementary RNA and DNA. *Biochemistry*, **43**, 13233–13241.
12. Nielsen,P.E., Egholm,M., Berg,R.H. and Buchardt,O. (1991) Sequence-selective recognition of DNA by strand displacement with a thymine-substituted polyamide. *Science*, **254**, 1497–1500.
13. Bentin,T., Hansen,G.I. and Nielsen,P.E. (2006) Structural diversity of target-specific homopyrimidine peptide nucleic acid-dsDNA complexes. *Nucleic Acids Res.*, **34**, 5790–5799.
14. Griffith,M.C., Risen,L.M., Greig,M.J., Lesnik,E.A., Sprankle,K.G., Griffey,R.H., Kiely,J.S. and Freier,S.M. (1995) Single and bis peptide nucleic acids as triplexing agents: binding and stoichiometry. *J. Am. Chem. Soc.*, **117**, 831–832.
15. Nielsen,P.E., Egholm,M. and Buchardt,O. (1994) Evidence for (PNA)2/DNA triplex structure upon binding of PNA to dsDNA by strand displacement. *J. Mol. Recogn.*, **7**, 165–170.
16. Kosaganov,Y.N., Stetsenko,D.A., Lubyako,E.N., Kvitko,N.P., Lazurkin,Y.S. and Nielsen,P.E. (2000) Effect of temperature and ionic strength on the dissociation kinetics and lifetime of PNA–DNA triplexes. *Biochemistry*, **39**, 11742–11747.
17. Demidov,V.V., Yavnilovich,M.V., Belotserkovskii,B.P., Frank-Kamenetskii,M.D. and Nielsen,P.E. (1995) Kinetics and mechanism of polyamide (''peptide'') nucleic acid binding to duplex DNA. *Proc. Natl Acad. Sci. USA*, **92**, 2637–2641.
18. Lohse,J., Dahl,O. and Nielsen,P.E. (1999) Double duplex invasion by peptide nucleic acid: a general principle for sequence-specific targeting of double-stranded DNA. *Proc. Natl Acad. Sci. USA*, **96**, 11804–11808.
19. Nielsen,P.E. and Christensen,L. (1996) Strand displacement binding of a duplex-forming homopurine PNA to a homopyrimidine duplex DNA target. *J. Amer. Chem. Soc.*, **118**, 2287–2288.
20. Sen,A. and Nielsen,P.E. (2006) Unique properties of purine/pyrimidine asymmetric PNA.DNA duplexes: differential stabilization of PNA.DNA duplexes by purines in the PNA strand. *Biophys. J.*, **90**, 1329–1337.

21. Rapireddy,S., He,G., Roy,S., Armitage,B.A. and Ly,D.H. (2007) Strand invasion of mixed-sequence B-DNA by acridine-linked, gamma-peptide nucleic acid (gamma-PNA). *J. Am. Chem. Soc.*, **129**, 15596–15600.
22. Bentin,T. and Nielsen,P.E. (1996) Enhanced peptide nucleic acid binding to supercoiled DNA: possible implications for DNA 'breathing' dynamics. *Biochemistry*, **35**, 8863–8869.
23. Cherny,D.Y., Belotserkovskii,B.P., Frank-Kamenetskii,M.D., Egholm,M., Buchardt,O., Berg,R.H. and Nielsen,P.E. (1993) DNA unwinding upon strand-displacement binding of a thymine-substituted polyamide to double-stranded DNA. *Proc. Natl Acad. Sci. USA*, **90**, 1667–1670.
24. Kuhn,H., Demidov,V.V., Frank-Kamenetskii,M.D. and Nielsen,P.E. (1998) Kinetic sequence discrimination of cationic bis-PNAs upon targeting of double-stranded DNA. *Nucleic Acids Res.*, **26**, 582–587.
25. Kurakin,A., Larsen,H.J. and Nielsen,P.E. (1998) Cooperative strand displacement by peptide nucleic acid (PNA). *Chem. Biol.*, **5**, 81–89.
26. Larsen,H.J. and Nielsen,P.E. (1996) Transcription-mediated binding of peptide nucleic acid (PNA) to double-stranded DNA: sequence-specific suicide transcription. *Nucleic Acids Res.*, **24**, 458–463.
27. Peffer,N.J., Hanvey,J.C., Bisi,J.E., Thomson,S.A., Hassman,C.F., Noble,S.A. and Babiss,L.E. (1993) Strand-invasion of duplex DNA by peptide nucleic acid oligomers. *Proc. Natl Acad. Sci. USA*, **90**, 10648–10652.
28. Kaihatsu,K., Braasch,D.A., Cansizoglu,A. and Corey,D.R. (2002) Enhanced strand invasion by peptide nucleic acid-peptide conjugates. *Biochemistry*, **41**, 11118–11125.
29. Bentin,T. and Nielsen,P.E. (2003) Superior duplex DNA strand invasion by acridine conjugated peptide nucleic acids. *J. Am. Chem. Soc.*, **125**, 6378–6379.
30. Janowski,B.A., Kaihatsu,K., Huffman,K.E., Schwartz,J.C., Ram,R., Hardy,D., Mendelson,C.R. and Corey,D.R. (2005) Inhibiting transcription of chromosomal DNA with antigene peptide nucleic acids. *Nat. Chem. Biol.*, **1**, 210–215.
31. Milne,L., Xu,Y., Perrin,D.M. and Sigman,D.S. (2000) An approach to gene-specific transcription inhibition using oligonucleotides complementary to the template strand of the open complex. *Proc. Natl Acad. Sci. USA*, **97**, 3136–3141.
32. Wittung,P., Nielsen,P. and Nordén,B. (1997) Extended DNA-recognition repertoire of peptide nucleic acid (PNA): PNA–dsDNA triplex formed with cytosine-rich homopyrimidine PNA. *Biochemistry*, **36**, 7973–7979.
33. Zhilina,Z.V., Ziemba,A.J., Nielsen,P.E. and Ebbinghaus,S.W. (2006) PNA-nitrogen mustard conjugates are effective suppressors of HER-2/neu and biological tools for recognition of PNA/DNA interactions. *Bioconj. Chem.*, **17**, 214–222.
34. Christensen,L., Fitzpatrick,R., Gildea,B., Petersen,K.H., Hansen,H.F., Koch,T., Egholm,M., Buchardt,O., Nielsen,P.E., Coull,J. *et al.* (1995) Solid-phase synthesis of peptide nucleic acids. *J. Pept. Sci.*, **1**, 175–183.
35. Sambrook,J. and Russel,D.W. (2001) *Molecular Cloning: a Laboratory Manual*. Cold Spring Harbor Laboratory Press.
36. Egholm,M., Christensen,L., Dueholm,K.L., Buchardt,O., Coull,J. and Nielsen,P.E. (1995) Efficient pH-independent sequence-specific DNA binding by pseudoisocytosine-containing bis-PNA. *Nucleic Acids Res.*, **23**, 217–222.
37. Brunet,E., Corgnali,M., Perrouault,L., Roig,V., Asseline,U., Sorensen,M.D., Babu,B.R., Wengel,J. and Giovannangeli,C. (2005) Intercalator conjugates of pyrimidine locked nucleic acid-modified triplex-forming oligonucleotides: improving DNA binding properties and reaching cellular activities. *Nucleic Acids Res.*, **33**, 4223–4234.
38. Gryaznov,S.M., Lloyd,D.H., Chen,J.K., Schultz,R.G., DeDionisio,L.A., Ratmeyer,L. and Wilson,W.D. (1995) Oligonucleotide N3′→P5′- phosphoramidates. *Proc. Natl Acad. Sci. USA*, **92**, 5798–5802.
39. Escude,C., Giovannangeli,C., Sun,J.S., Lloyd,D.H., Chen,J.K., Gryaznov,S.M., Garestier,T. and Helene,C. (1996) Stable triple helices formed by oligonucleotide N3′→P5′ phosphoramidates inhibit transcription elongation. *Proc. Natl Acad. Sci. USA*, **93**, 4365–4369.
40. Rusling,D.A., Powers,V.E., Ranasinghe,R.T., Wang,Y., Osborne,S.D., Brown,T. and Fox,K.R. (2005) Four base recognition by triplex-forming oligonucleotides at physiological pH. *Nucleic Acids Res.*, **33**, 3025–3032.
41. Shiraishi,T., Hamzavi,R. and Nielsen,P.E. (2005) Targeted delivery of plasmid DNA into the nucleus of cells via nuclear localization signal peptide conjugated to DNA intercalating bis- and trisacridines. *Bioconjug. Chem.*, **16**, 1112–1116.